Mineralogical Magazine, June 2015, Vol. 79(3), pp. 687–694

Eckerite, Ag_2CuAsS_3, a new Cu-bearing sulfosalt from Lengenbach quarry, Binn valley, Switzerland: description and crystal structure

L. Bindi[1,2,*], F. Nestola[3], S. Graeser[4], P. Tropper[5] and T. Raber[6]

[1] Dipartimento di Scienze della Terra, Università degli Studi di Firenze, Via G. La Pira 4, I-50121 Firenze, Italy
[2] CNR – Istituto di Geoscienze e Georisorse, Sezione di Firenze, Via G. La Pira 4, I-50121 Firenze, Italy
[3] Dipartimento di Geoscienze, Università degli Studi di Padova, Via Gradenigo 6, I-35131 Padova, Italy
[4] Mineralogisches Institut, Universität Basel, Bernoullistrasse 30, CH-4056 Basel, Switzerland
[5] Institute of Mineralogy and Petrography, University of Innsbruck, Innrain 52f, A-6020 Innsbruck, Austria
[6] FGL (Forschungsgemeinschaft Lengenbach), Edith-Stein-Strasse 9, D-79110 Freiburg, Germany

[*Received 6 October 2014; Accepted 7 December 2014; Associate Editor: A. Christy*]

ABSTRACT

Eckerite, ideally Ag_2CuAsS_3, is a new mineral from the Lengenbach quarry in the Binn Valley, Valais, Switzerland. It occurs as very rare euhedral crystals up to 300 μm across associated with realgar, sinnerite, hatchite, trechmannite and yellow, fibrous smithite. In thick section eckerite is opaque with a metallic lustre and shows a dark orange-red streak. It is brittle; the Vickers hardness (VHN_{25}) is 70 kg/mm^2 (range: 64–78) (Mohs hardness of ~2½–3). In reflected light, eckerite is moderately bireflectant and weakly pleochroic from light grey to a slightly bluish grey. Internal reflections are absent. Under crossed nicols, it is weakly anisotropic with greyish to light blue rotation tints. Reflectance percentages for R_{min} and R_{max} are 27.6, 31.7 (471.1 nm), 22.8, 26.1 (548.3 nm), 21.5, 24.5 (586.6 nm) and 19.4, 22.3 (652.3 nm), respectively.

Eckerite is monoclinic, space group $C2/c$, with a = 11.8643(3), b = 6.2338(1), c = 16.6785(4) Å, β = 110.842(3)°, V = 1152.81(5) Å^3, Z = 8. The crystal structure [R_1 = 0.0769 for 1606 reflections with $F_o > 4\sigma(F_o)$] is topologically identical to that of xanthoconite and pyrostilpnite. In the structure, AsS_3 pyramids are joined by AgS_3 triangles to form double sheets parallel to (001); the sheets are linked by Cu(Ag) atoms in a quasi-tetrahedral coordination. Among the three metals sites, Ag2 is dominated by Cu. The mean metal–S distances reflect well the Ag ↔ Cu substitution occurring at this site.

The eight strongest powder X-ray diffraction lines [d in Å (I/I_0) (hkl)] are: 3.336 (70) ($\bar{3}12$); 2.941 (100) ($\bar{3}14$,114); 2.776 (80) (400,$\bar{2}06$); 2.677 (40) (312); 2.134 (50) ($\bar{4}21$); 2.084 (40) ($\bar{2}08$,206); 2.076 (40) (420); 1.738 (40) ($\bar{2}28$,226). A mean of five electron microprobe analyses gave Ag 52.08(16), Cu 11.18(9), Pb 0.04(1), Sb 0.29(3), As 15.28(11), S 20.73(13), total 99.60 wt.%, corresponding, on the basis of a total of 7 atoms per formula unit, to $Ag_{2.24}Cu_{0.82}As_{0.94}Sb_{0.01}S_{2.99}$. The new mineral has been approved by the International Mineralogical Association Commission on New Minerals, Nomenclature and Classification (2014–063) and named for Markus Ecker, a well known mineral expert on the Lengenbach minerals for more than 25 years.

Keywords: eckerite, new mineral, Ag-sulfosalts, Lengenbach, Switzerland.

Introduction

The Lengenbach quarry, the type locality for 32 new mineral species (Roth *et al*., 2014), exploits a Triassic dolostone overlying gneiss basement, at the northern front of the Monte Leone Nappe in

---

* E-mail: luca.bindi@unifi.it
DOI: 10.1180/minmag.2015.079.3.13

the Penninic domain of the Alps. The rocks were metamorphosed to upper greenschist–lower amphibolite facies. The dolostone is 240 m thick at Lengenbach; mineralization occurs in the uppermost part of the sequence, 180 to 200 m above its base, close to the contact with the overlying Jurassic to Lower Cretaceous 'Bündnerschiefer'. Hofmann and Knill (1996) recognized four major types of mineralization; stratiform layers of pyrite, with minor galena, sphalerite and xenomorphic sulfosalts; massive to interstitial sulfosalt accumulations; discordant sulfosalt and sulfide veins; and idiomorphic minerals within druses and open fissures. Eckerite was observed in the second type of mineralization, corresponding to the "Zone 1" of Graeser *et al*. (2008), on a sample with the official number L-27381 of the AGL [*Arbeitsgemeinschaft Lengenbach* (Lengenbach Working Association), active from 1958 until 1997]. The dolomite in this zone shows a very saccharoidal texture. It hosts the largest pyrite concentration and baumhauerite, sartorite and realgar are the main arsenic mineral phases present. Minerals associated with eckerite are realgar, sinnerite, hatchite, trechmannite and yellow, fibrous smithite.

Eckerite was approved as a new mineral by the Commission on New Minerals, Nomenclature and Classification of the International Mineralogical Association (2014-063, Bindi *et al*., 2015). The mineral name honours Markus Ecker (b. 1966), a well known mineral expert on the Lengenbach minerals for more than 25 years. He has found several new mineral species from Lengenbach and has published many articles about the quarry and its minerals. He is currently a Member of the Technical Commission of the *Forschungsgemeinschaft Lengenbach* (FGL, Lengenbach Research Association).

The holotype material is deposited in the mineralogical collections of the Museo di Storia Naturale, Università degli Studi di Firenze, Italy (under catalogue number 3144/I) and at the Natural History Museum, University of Basel, Switzerland (under catalogue number S169).

In this study we report the description of the new mineral eckerite together with the determination of its crystal structure.

Physical and optical properties

Eckerite occurs as very rare crystals growing on dolomite, sometimes growing on smithite or sinnerite (Fig. 1). The mineral exhibits a subhedral to anhedral grain morphology, and shows no inclusions of, or intergrowths with, other minerals. The maximum grain size of eckerite is ~300 μm.

In thin plates, the mineral is transparent and red in colour, it shows an orange-red streak and an adamantine lustre. On the contrary, in thick sections it is opaque in transmitted light and exhibits a metallic lustre. No cleavage is observed and the fracture is irregular. The calculated density (for $Z = 8$) for the empirical formula (see below) is 5.313 g/cm^3. Unfortunately, the density could not be measured because of the small grain size. Micro-indentation measurements carried out with a VHN load of 25g give a mean value of 70 kg/mm^2 (range: 64–78) corresponding to a Mohs hardness of ~2½–3.

In plane-polarized incident light, eckerite is moderately bireflectant and weakly pleochroic from light grey to a slightly bluish grey. The mineral shows no internal reflections. Between crossed nicols, eckerite is weakly anisotropic with greyish to light-blue rotation tints.

Reflectance measurements were performed in air by means of a MPM-200 Zeiss microphotometer equipped with a MSP-20 system processor on a Zeiss Axioplan ore microscope. The filament temperature was ~3350 K. An interference filter was adjusted, sequentially, to select four wavelengths for measurement (471.1, 548.3, 586.6 and 652.3 nm). Readings were taken for specimen and standard (SiC) maintained under the same focus conditions. The diameter of the circular measuring area was 0.1 mm. Reflectance percen-

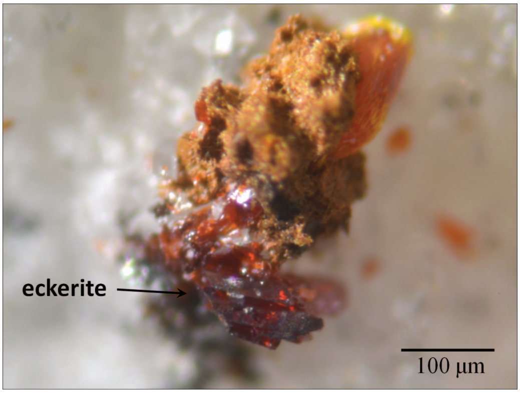

FIG. 1. Eckerite (reddish-brown) in association with yellowish, fibrous smithite and realgar.

TABLE 1. Data and experimental details for the selected eckerite crystal.

Crystal data	
Formula	Ag_2CuAsS_3
Crystal size (mm)	0.080 × 0.090 × 0.110
Form	block
Colour	red
Crystal system	Monoclinic
Space group	$C2/c$ (#15)
a (Å)	11.8643(3)
b (Å)	6.2338(1)
c (Å)	16.6785(4)
β (º)	110.842(3)
V (Å^3)	1152.81(5)
Z	8
Data collection	
Instrument	STOE-STADI IV CCD
Radiation type	Mo$K\alpha$ (λ = 0.71073 Å)
Temperature (K)	293(3)
Detector-to-sample distance (cm)	5
Number of frames	1563
Measuring time (s)	40
Maximum covered 2θ (º)	69.26
Collected reflections	17,445
Unique reflections	2488
Reflections with $F_o > 4\sigma(F_o)$	1606
R_{int}	0.0581
R_σ	0.0355
Range of h, k, l	$-18 \leqslant h \leqslant 18$, $-10 \leqslant k \leqslant 10$, $-26 \leqslant l \leqslant 26$
Refinement	
Refinement	Full-matrix least squares on F^2
Final R_1 [$F_o > 4\sigma(F_o)$]	0.0769
Final R_1 (all data)	0.0825
Number refined parameters	67
$\Delta\rho_{max}$ (e Å^{-3})	3.76
$\Delta\rho_{min}$ (e Å^{-3})	−3.59

tages for R_{min} and R_{max} are 27.6, 31.7 (471.1 nm), 22.8, 26.1 (548.3 nm), 21.5, 24.5 (586.6 nm) and 19.4, 22.3 (652.3 nm), respectively.

X-ray crystallography and crystal-structure determination

A crystal fragment (80 μm × 90 μm × 110 μm) was selected for the X-ray single-crystal diffraction study that was undertaken with a STOE-STADI IV CCD single-crystal diffractometer (Table 1). Data were integrated and corrected for standard Lorentz polarization factors with the *CrysAlis RED* (Oxford Diffraction, 2006) software package. The program *ABSPACK* in *CrysAlis RED* (Oxford Diffraction, 2006) was used for the absorption correction. The observed reflection conditions (hkl: $h+k = 2n$; $h0l$: $h,l = 2n$; $0kl$: $k = 2n$; $hk0$: $h+k = 2n$; $0k0$: $k = 2n$; $h00$: $h = 2n$; $00l$: $l = 2n$), together with the statistical tests on the distribution of $|E|$ values that strongly indicated the presence of an inversion centre ($|E^2 - 1| = 0.896$), pointed to the choice of the space group $C2/c$. The structure solution was then initiated in this space group. The positions of most of the atoms (all the metal positions and most of the S atoms) were determined by means of direct methods (Sheldrick, 2008). A least-squares refinement on F^2 using these heavy-atom positions and isotropic temperature factors produced an R factor of 0.134. Three-dimensional difference Fourier synthesis yielded the positions

TABLE 2. Atom, site occupancy factors (s.o.f.), fractional atom coordinates and equivalent isotropic atomic displacement parameters (Å^2) for eckerite.

Atom	s.o.f.	*x*/*a*	y/*b*	z/*c*	U_{eq}
Ag1	$Ag_{0.84(2)}Cu_{0.16}$	0.1431(2)	0.0350(3)	0.21371(9)	0.0668(8)
Ag2	$Ag_{0.37(2)}Cu_{0.63}$	0.0586(2)	0.9218(5)	0.4328(2)	0.084(1)
Ag3	$Ag_{1.00}$	0.3596(1)	0.0264(3)	0.1354(2)	0.0776(7)
As	$As_{1.00}$	0.3536(1)	0.0463(2)	0.43332(8)	0.0258(3)
S1	$S_{1.00}$	0.1513(3)	0.1797(5)	0.0765(2)	0.0372(7)
S2	$S_{1.00}$	0.4260(3)	0.1404(6)	0.3294(2)	0.0347(7)
S3	$S_{1.00}$	0.1573(3)	0.1253(5)	0.3600(2)	0.0343(7)

of the remaining sulfur atoms. The program *SHELXL* (Sheldrick, 2008) was used for the refinement of the structure. The occupancy of all the sites was left free to vary (Ag *vs*. Cu for the Ag sites; As *vs*. Sb; S *vs*. vacancy). The occupancy of Ag3, As and the S sites was found to be consistent with a pure occupation by Ag, As and S, respectively, and then fixed. Neutral scattering curves for Ag, Cu, As, Sb and S were taken from the *International Tables for X-ray Crystallography* (Ibers and Hamilton, 1974). At the last stage, with anisotropic atomic displacement parameters for all atoms and no constraints (except the named occupancies), the residual value settled at R_1 = 0.0769 for 1606 observed reflections [$F_o > 4\sigma(F_o)$ level] and 67 parameters and at R_1 = 0.0825 for all 2488 independent reflections. Inspection of the difference Fourier map revealed that maximum positive and negative peaks were 3.76 and 3.59 e$^-$/Å^3, respectively. Experimental details and *R* indices are given in Table 1. Fractional atomic coordinates and isotropic displacement parameters are reported in Table 2 whereas the anisotropic displacement parameters are given in Table 3. Bond distances are given in Table 4. The calculated powder X-ray diffraction pattern, computed with the atom coordinates and occupancies reported in Table 2, is given in Table 5 together with the measured pattern (114.6 mm diameter Gandolfi camera, Fe*K*α radiation). Unit-cell parameters refined from the powder data are: *a* = 11.871(6), *b* = 6.2251(3), *c* = 16.635(7) Å, β = 110.89(2)º, *V* = 1158.6(5) Å^3.

Structure factors (Table 6) have been deposited with the Principal Editor of *Mineralogical Magazine* and are available at http://www.minersoc.org/pages/e_journals/dep_mat_mm.html.

Chemical composition

A preliminary chemical analysis using energy dispersive spectroscopy performed on the crystal fragment used for the structure study did not indicate the presence of elements ($Z > 9$) other than Ag, Cu, As and S. The chemical composition was then determined using wavelength dispersive analysis (WDS) by means of a JEOL 8100 SUPERPROBE electron microprobe. Major and

TABLE 3. Anisotropic atomic displacement parameters (Å^2) for eckerite.

	U_{11}	U_{22}	U_{33}	U_{12}	U_{13}	U_{23}
Ag1	0.070(1)	0.088(2)	0.0403(9)	−0.0109(9)	0.0159(7)	−0.0060(7)
Ag2	0.047(1)	0.119(2)	0.069(2)	−0.030(1)	−0.0009(9)	0.053(1)
Ag3	0.0335(7)	0.0460(8)	0.144(2)	−0.0004(5)	0.0193(8)	0.0002(9)
As	0.0252(5)	0.0247(6)	0.0275(6)	−0.0022(4)	0.0095(4)	−0.0013(4)
S1	0.033(2)	0.024(1)	0.054(2)	−0.001(1)	0.015(1)	−0.005(1)
S2	0.032(2)	0.041(2)	0.034(2)	0.001(1)	0.017(1)	0.004(1)
S3	0.024(1)	0.031(1)	0.048(2)	0.001(1)	0.012(1)	0.001(1)

TABLE 4. Selected bond distances (Å) for eckerite.

Ag1–S3	2.451(4)	Ag2–S3	2.338(4)	Ag3–S2	2.502(4)	As–S3	2.266(3)
S1	2.494(4)	S1	2.341(4)	S1	2.501(4)	S2	2.268(3)
S2	2.612(4)	S2	2.568(4)	S3	2.512(4)	S1	2.291(3)
mean	2.519	S2	2.922(5)	mean	2.505	mean	2.275
		mean	2.542				

TABLE 5. Measured and calculated powder X-ray diffraction data for eckerite.

	— (*a*) —		— (*b*) —	
hkl	d_{meas}	I_{est}	d_{calc}	I_{calc}
$\bar{1}11$	5.444	10	5.4341	6
112	4.148	10	4.1322	20
202			3.9083	5
	3.893	20		
004			3.8967	20
$\bar{3}12$	3.336	70	3.3204	38
310	3.195	10	3.1792	8
$\bar{3}14$			2.9438	100
	2.941	100		
114			2.9337	97
400			2.7720	74
	2.776	80		
$\bar{2}06$			2.7596	46
312	2.677	40	2.6716	26
$\bar{2}23$	2.606	20	2.6011	11
$\bar{4}06$	2.348	10	2.3602	8
$\bar{4}21$	2.134	50	2.1285	19
$\bar{2}08$			2.0847	17
	2.084	40		
206			2.0846	21
420	2.076	40	2.0714	29
404			1.9541	12
	1.949	20		
008			1.9484	2
132			1.9447	12
$\bar{2}27$	1.893	10	1.8915	20
133			1.8598	16
	1.851	10		
$\bar{6}06$			1.8481	17
$\bar{2}28$			1.7329	9
	1.738	40		
226			1.7328	17
227			1.5915	9
	1.595	30		
$\bar{6}26$			1.5897	9
$\bar{1}1\overline{10}$	1.573	10	1.5727	17
626	1.204	10	1.2020	4

(*a*) = measured Gandolfi diffraction pattern (Fe*K*α); (*b*) = diffraction pattern calculated for Fe*K*α using the atom coordinates and site occupancies reported in Table 2.

minor elements were determined at 20 kV accelerating voltage and 10 nA beam current, 1 μm beam size and with counting times of 20 s for peak and 10 s for background. For the WDS analyses the *K*α lines for all the elements were used. The standards employed were: Ag-pure element (Ag), Cu-pure element (Cu), galena (Pb), Sb-pure element (Sb), As-pure element (As) and troilite (S). The crystal fragment was found to be homogeneous within analytical error. The average chemical compositions (five analyses on different spots) together with wt.% ranges of elements are reported in Table 7. On the basis of 7 atoms, the empirical formula of eckerite is $Ag_{2.24}Cu_{0.82}As_{0.94}Sb_{0.01}S_{2.99}$, which is in excellent agreement with that obtained from the structure refinement, $Ag_{2.21}Cu_{0.79}AsS_3$. The simplified formula is Ag_2CuAsS_3, which requires Ag 47.90, Cu 14.11, As 16.63, S 21.36, total 100.00 wt.%.

Results and discussion

Description of the structure

The crystal structure of eckerite (Fig. 2) is topologically identical to that of xanthoconite (Engel and Nowacki, 1968) and pyrostilpnite (Kutoglu, 1968), with one of three independent Ag positions dominated by Cu (i.e. Ag2). In the structure, AsS_3 pyramids are joined by AgS_3 triangles to form double sheets parallel to (001); the sheets are linked by the metal position dominated by copper in a quasi-tetrahedral coordination. The mean bond distances for the three-coordinated Ag-polyhedra (Ag1 and Ag3) are in the range 2.45–2.61 Å (Table 4), which matches well those observed for triangularly-coordinated Ag atoms in the different polytypes of the pearceite–polybasite minerals (2.43–2.62 Å, Bindi *et al.*, 2006, 2007; Evain *et al.*, 2006). The Ag2 position dominated by Cu in eckerite shows a quasi-tetrahedral coordination with a mean bond distance of 2.542 Å compared to 2.674 Å in Cu-free xanthoconite (Engel and Nowacki, 1968). The ordering of copper mainly at

TABLE 7. Electron microprobe data (means and ranges in wt.% of elements), atomic ratios (on the basis of 7 atoms per formula unit) with their standard deviations (σ) for the selected eckerite crystal.

	Wt.%	Range	Atomic ratios	Σ
Ag	52.08	50.63–52.83	2.24	0.16
Cu	11.18	10.73–11.82	0.82	0.09
Pb	0.04	0.00–0.10	0.00	0.01
Sb	0.29	0.22–0.34	0.01	0.03
As	15.28	15.15–15.63	0.94	0.11
S	20.73	20.30–21.05	2.99	0.13
Total	99.60	99.44–99.82		

the Ag2 site in the eckerite structure reflects the preference of Cu for tetrahedral environments. Indeed, copper is usually hosted in tetrahedra in Cu sulfosalts [e.g. enargite (Karanovic *et al.*, 2002); luzonite (Pfitzner and Bernert, 2004); sinnerite (Bindi *et al.*, 2013)]. The shortest Ag–Ag contact in the eckerite structure is Ag1–Ag2 at 2.835 Å, slightly shorter than that found in *fcc* Ag metal (2.889 Å; Suh *et al.*, 1988).

Bond-valence sums calculated from the data of Brese and O'Keeffe (1991) are reported in Table 8. The valence sums obtained are in near-perfect agreement with the cation populations assumed in the present study.

Eckerite as a Cu-rich member of the xanthoconite–pyrostilpnite series

As is well known, Ag-Cu sulfosalts are an important source of silver and occur in a variety of hydrothermal ore deposits, in particular fissure-vein polymetallic base-metal sulfide deposits (e.g. Loucks and Petersen, 1988; Chutas and Sack, 2004). Among these sulfosalts, some of the most important are the proustite (Ag_3AsS_3)–pyrargyrite (Ag_3SbS_3) solid solution series, together with that between xanthoconite and pyrostilpnite, the rare low-temperature polymorphs (e.g. Lange *et al.*, 1993). Eckerite is structurally identical to these two latter minerals.

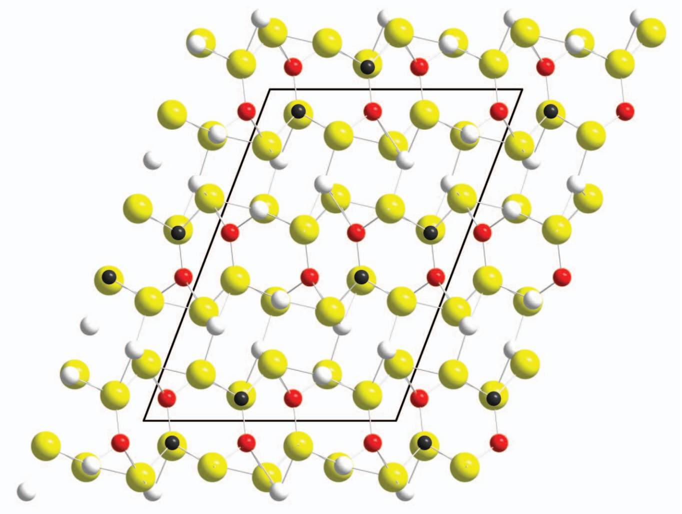

FIG. 2. The crystal structure of eckerite projected down [010]. The horizontal direction is the *a* axis. Ag, Cu (Ag2 position), As and S are given as white, red, black and yellow spheres, respectively. The unit cell is outlined.

TABLE 8. Bond valence (vu) calculation for eckerite*.

Atom	Bond valence
Ag1	0.978(5)
Ag2	1.003(5)
Ag3	1.057(5)
As	2.977(4)
S1	2.113(5)
S2	1.944(5)
S3	2.138(5)

* Calculated from the bond-valence parameters of Brese and O'Keeffe (1991). For Ag1 and Ag2 sites the weighted sums $Ag_{1-x}Cu_x$ (x = occupancy of Cu) of the bond-valence parameters were used.

Given the importance of these minerals in economic geology, a lot of attention has been paid to the mixing properties of these solid solutions. Bindi *et al.* (2010) have studied the crystallographic and chemical constraints on the proustite–pyrargyrite solid solution series by evaluating 32 natural samples of proustite and 27 samples of pyrargyrite. Interestingly, no Cu was detected in all the samples investigated. The same has been observed for the minerals of the xanthoconite–pyrostilpnite series, where Cu is only reported as a trace element (Gaines *et al.*, 1997). The lack of copper in minerals of the system proustite–pyrargyrite has been explained with thermodynamic considerations by Harlov and Sack (1995) and Harlov (1999). On the one hand, these authors showed that mixing on the As−Sb site is non-ideal and symmetric, and that complete solid solution occurs down to ~105ºC, and perhaps as low as 90ºC. On the other hand, they also pointed out that the mixing on the As−Sb site in proustite–pyrargyrite is more symmetric and more ideal than that for mixing on Cu−Ag sites, where it is both asymmetric and significantly non-ideal (Harlov and Sack, 1995; Harlov, 1999). The studies by Harlov (1999) reinforce the earlier investigation by Harlov and Sack (1995) that shows the greater stability of Ag when compared to Cu on the Ag−Cu sites for both proustite and pyrargyrite. Although eckerite belongs to the xanthoconite−pyrostilpnite series, we think that similar thermodynamic considerations can be applied. This would explain the rarity of eckerite and would justify why the mineral had not been discovered until now. The exceptional conditions needed to form such a unique phase emphasize the geochemical distinctiveness of the Lengenbach deposit, able to produce rare minerals not discovered in other deposits.

Acknowledgements

The paper benefited from reviews by Tonči Balić-Žunić, Peter Leverett and one anonymous reviewer. Associate Editor Andrew G. Christy is thanked for efficient handling of the manuscript. Martina Tribus is thanked for help with microprobe analysis. The research was supported by "progetto d'Ateneo 2012, University of Firenze" to LB.

References

Bindi, L., Evain, M. and Menchetti, S. (2006) Temperature dependence of the silver distribution in the crystal structure of natural pearceite, $(Ag,Cu)_{16}(As,Sb)_2S_{11}$. *Acta Crystallographica*, **B62**, 212−219.

Bindi, L., Evain, M. and Menchetti, S. (2007) Complex twinning, polytypism and disorder phenomena in the crystal structures of antimonpearceite and arsenpolybasite. *The Canadian Mineralogist*, **45**, 321−333.

Bindi, L., Pratesi, G. and Spry, P.G. (2010) Crystallographic and chemical constraints on the nature of the proustite-pyrargyrite solid solution series. *American Mineralogist*, **95**, 1725−1729.

Bindi, L., Makovicky, E., Nestola, F. and De Battisti, L. (2013) Sinnerite, $Cu_6As_4S_9$, from Lengenbach quarry, Binn valley, Switzerland: Description and re-investigation of the crystal structure. *The Canadian Mineralogist*, **51**, 851−860.

Bindi, L., Nestola, F., Graeser, S., Tropper, P. and Raber, T. (2015) Eckerite, IMA 2014-063. CNMNC Newsletter No. 23, February 2015, page 52; *Mineralogical Magazine*, **79**, 51−58.

Brese, N.E. and O'Keeffe, M. (1991) Bond-valence parameters for solids. *Acta Crystallographica*, **B47**, 192−197.

Chutas, N.I. and Sack, R.O. (2004) Ore genesis at La Colorada Ag-Zn-Pb deposit in Zacatecas, Mexico. *Mineralogical Magazine*, **68**, 923−937.

Engel, P. and Nowacki, W. (1968) Die Kristallstruktur von Ag_3AsS_3. *Acta Crystallographica*, **B24**, 77−81.

Evain, M., Bindi, L. and Menchetti, S. (2006) Structural complexity in minerals: twinning, polytypism and disorder in the crystal structure of polybasite, $(Ag,Cu)_{16}(Sb,As)_2S_{11}$. *Acta Crystallographica*, **B62**, 447−456.

Gaines, R.V., Skinner, H.C.W., Foord, E.E., Mason, B. and Rosenzweig, A. (1997) *Dana's New Mineralogy*.

8th Edition. John Wiley & Sons, New York, USA.

Graeser, S., Cannon, R., Drechsler, E., Raber, T. and Roth, P. (2008) *Faszination Lengenbach Abbau-Forschung-Mineralien 1958–2008*. Kristallographik Verlag, Achberg, Germany.

Harlov, D.E. (1999) Thermochemistry of Ag-Cu exchange equilibria between proustite, sinnerite, and pearceite: Constraints on Ag-Cu and As-Sb mixing in pyrargyrite-proustite. *European Journal of Mineralogy*, **11**, 709–719.

Harlov, D.E. and Sack, R.O. (1995) Thermochemistry of Ag_2S–Cu_2S sulfide solutions: Constraints derived from coexisting Sb_2S_3- and As_2S_3-bearing sulfosalts. *Geochimica et Cosmochimica Acta*, **59**, 4351–4365.

Hofmann, B.A. and Knill, M.D. (1996) Geochemistry and genesis of the Lengenbach Pb-Zn-As-Tl-Ba mineralization, Binn Valley, Switzerland. *Mineralium Deposita*, **31**, 319–339.

Ibers, J.A. and Hamilton, W.C. (editors) (1974) *International Tables for X-ray Crystallography, Vol. 4*. Kynock, Dordrecht, The Netherlands, pp. 366.

Karanovic, L., Cvetkovic, L., Poleti, D., Balić-Žunić, T. and Makovicky, E. (2002) Crystal and absolute structure of enargite from Bor (Serbia). *Neues Jahrbuch für Mineralogie, Monatshefte*, **2002**, 241–253.

Kutoglu, A. (1968) Die Struktur des Pyrostilpnits (Feuerblende) Ag_3SbS_3. *Neues Jahrbuch für Mineralogie, Monatshefte*, 145–160.

Lange, B., Scholz, F., Bautsch, H.-J., Damaschun, F. and Wappler, G. (1993) Thermodynamics of the xanthoconite-proustite and pyrostilpnite-pyrargyrite phase transition as determined by abrasive stripping voltammetry. *Physics and Chemistry of Minerals*, **19**, 486–491.

Loucks, R.R. and Petersen, U. (1988) Polymetallic epithermal fissure vein mineralization, Topia, Durango, Mexico: Part II. Silver mineral chemistry and high resolution patterns of chemical zoning in veins. *Economic Geology*, **83**, 1529–1559.

Oxford Diffraction (2006) *CrysAlis RED (Version 1.171.31.2)* and *ABSPACK* in *CrysAlis RED*. Oxford Diffraction Ltd, Abingdon, Oxfordshire, England.

Pfitzner, A. and Bernert, T. (2004) The system Cu_3AsS_4–Cu_3SbS_4 and investigations on normal tetrahedral structures. *Zeitschrift für Kristallographie*, **219**, 20–26.

Roth, P., Raber, T., Drechsler, E. and Cannon, R. (2014) The Lengenbach quarry, Binn Valley, Switzerland. *Mineralogical Record*, **45**, 157–196.

Sheldrick, G.M. (2008) A short history of SHELX. *Acta Crystallographica*, **A64**, 112–122.

Suh, In-Kook, Ohta, H. and Waseda, Y. (1988) High-temperature thermal expansion of six metallic elements measured by dilatation method and X-ray diffraction. *Journal of Materials Science*, **23**, 757–760.